Photosensitivity of SiO_2–Al and SiO_2–Na glasses under ArF (193 nm) laser

A.N. Trukhin [a,*], J. Teteris [a], A. Fedotov [a], D.L. Griscom [b], G. Buscarino [c]

[a] Solid State Physics Institute, University of Latvia, Kengaraga, 8, LV-1063 Riga, Latvia
[b] Impactglass Research International, 3938 E. Grant Rd. #131, Tucson, AZ 85712, USA
[c] Istituto Nazionale per la Fisica della Materia and Dipartimento di Scienze Fisiche ed Astronomiche dell'Università, via Archirafi, 36, I-90123 Palermo, Italy

ARTICLE INFO

ABSTRACT

Photosensitivity of SiO_2–Al and SiO_2–Na glass samples was probed by means of the induced optical absorption and luminescence as well as by electron spin-resonance (ESR) after irradiation with excimer-laser photons (ArF, 193 nm). Permanent visible darkening in the case of SiO_2–Al and transient, life time about one hour, visible darkening in the case of SiO_2–Na was found under irradiation at 290 K. No darkening was observed at 80 K for either kind of material. This investigation is dedicated to revealing the electronic processes responsible for photosensitivity at 290 and 80 K. The photosensitivity of both materials is related to impurity defects excited directly in the case of SiO_2–Na and/or by recapture of self-trapped holes, which become mobile at high temperature in the case of SiO_2–Al. Electrons remain trapped on the localized states formed by oxygen deficient defects.

© 2009 Elsevier B.V. All rights reserved.

1. Introduction

One of the general properties of glassy state is the existence of localized electronic states, which survive separately from the band structure usual for electronic states of all solid materials. The valence band and conduction band remain; however, the band structure as dispersion of energy within the space of quasi-impulse loses is meaning with respect to crystal. After Mott's definition, localized states are similar to traps in crystals, with no transport between these states in spite of wave function overlap [1].

The photosensitivity of many materials is based on processes involving localized states. A good example is the class of semi-conducting materials [2]. For these materials in the crystalline state the general characteristic is the large dimension of the electronic excitation, several tens of the inter-atom distance. In the amorphous state the dimension of electronic excitation falls to the value of the distance between atoms and is specific to defects of low radius appearing in material. Localized states are connected with those defects.

Wide gap insulating materials are characterized by low values of the electronic excitation dimensions, even in the crystalline case. Therefore, many properties of these materials are not affected in principal by vitrification. For example, the fundamental absorption range of crystalline and glassy silicon dioxide possesses

* Corresponding author. Tel.: +371 67260 686; fax: +371 67132778.
E-mail address: truhins@latnet.lv (A.N. Trukhin).

similar spectra [3]. This gives rise to difficulties for determining the localized states in the corresponding glassy modifications of materials. In the case of wide-gap insulators, it can be difficult to define the boundary between localized states and the excited states of the component defects. In some cases of some two-component glasses, such as sodium silicates, it has been possible to resolve the localized states, because in these materials these states are mainly connected with the sodium oxide sub-lattice (see e.g. [4]). The sodium oxide sub-lattice provides electronic states lower than that of silicon dioxide sub lattice. All processes relating to localized states are developed in sodium oxide sub-lattice [4].

As-received pure (OH-free) oxidized silicon dioxide glass exhibits very low absorption below optical gap. Only oxygen deficient pure silica glass possesses optical absorption below the gap after material preparation, which has been demonstrated by measurements of a specific luminescence [4,5]. Communities of these oxygen deficient defects form the localized states of silica glass responsible for much of the optical absorption below the gap. These localized states of silica glass are connected with oxygen deficient center of luminescence and are likely affiliated with structural motifs different from tetrahedral, because the corresponding oxygen deficient center of this luminescence as never been observed in α-quartz crystals, whereas it has been observed in silicon dioxide crystals with rutile structure (stishovite) [6]. The analogous situation is observed in germanium dioxide glasses and rutile-like GeO_2 crystals [7]. Oxygen deficiency in tetrahedral structures provides precursors of the E'-centers [8].

Photosensitivity of pure silica glass resulting from accumulation of charge carriers in traps [5,9] is directly connected with the level of oxygen deficiency. Photosensitivity of silica glass increases significantly with doping [10,11]. In many cases, (see e.g. [10,11] and references therein) role of aluminum co-doped with alkali ion was studied. Tetrahedrally coordinated Al plays the role of a hole trap and it is presumed, as rule, that alkali ions play the role of electron trap. Now we have studied the influences of Al or Na doping of silica separately. It was found that under pulses of ArF laser light (193 nm) visible coloration appears in both cases. However, the Al-doped samples exhibited coloration stable at room temperature, whereas the coloration the Na doped sample decreased to initial level within 1–2 h. The task of the present study is to achieve an understanding of the mechanisms of electron trapping in Al and Na-doped silica glass samples under ArF laser irradiation and their relationships to localized states of silica. It is assumed that knowledge of such processes should be useful for interpretation of others cases of photosensitivity in glasses.

2. Experimental

The samples of this investigation were silica glasses doped with 0.01, 0.025, and 0.05 wt% of Al_2O_3 prepared by adding to synthetic silicon dioxide powder before electrofusion. The samples with sodium were made by the same method to have concentrations 0.025 and 0.05 wt% of Na_2O.

The ArF laser (193 nm), model PSX-100, was made by Neweks, Estonia and has a pulse energy of about 5 mJ with a duration of 5 ns. Luminescence detection was realized by means of a grating monochromator (MCD-1) having both slits about 1 mm, with a photomultiplier tube(H6780-04) with 50 Ω resistive load. An oscilloscope (Tektronic TDS 2022B) was exploited for decay curve registration. Each curve was averaged for 128 pulses. The time-resolved spectra were measured by registration of the decay curve for each point of the PL spectrum in two time ranges – one in the nanosecond range another in the millisecond range. Measurement of afterglow during several hundreds of a second was performed by means of a photon counting method with a photomultiplier (FEU-

106). The measured curves are presented in the figures without smoothing and therefore reflect the level of errors. The absorption spectra were measured on two different spectrometers. One was an Ocean Optics mini-spectrometer working in the range 1000–220 nm, another was a spectrometer based on a 70° Seya-Namioka vacuum monochromator with deuterium discharge light source. The measured spectra are stitched together at 220 nm. The samples were irradiated with the ArF laser for half an hour with pulse frequency 11 Hz.

ESR spectra recorded in Riga were recorded in the slow-passage first-derivative mode on an analog RE-1307 X-band (9 GHz) spectrometer with magnetic field modulation at 100 Hz. The samples were measured before and after irradiation with ArF laser light in air at 290 K or immersed in liquid nitrogen in a quartz-glass Dewar. The ArF-irradiated samples were transferred to another quartz-glass Dewar for ESR measurement at 80 K. Samples with prior radiation histories were cleansed of previously induced defects by annealing to 900 K prior to laser exposure.

Additional ESR experiments, including some spectra recorded in the fast-passage high-power second-harmonic mode [12] were carried out in Palermo on a computer-controlled Bruker EMX spectrometer. In these cases only room temperature measurements were recorded.

3. Results

The optical absorption spectra of the studied samples are presented in Figs. 1 and 2. Irradiation with ArF laser pulses makes changes in absorption spectra in a wide spectral range. Several optical absorption bands due to induced color centers appeared at 2.25, 4.1, 5.5, 6.4 and 7.6 eV under ArF laser at 290 K in Al containing sample. These bands do not appear for irradiation at 80 K; rather, only structureless induced absorption increasing up to optical gap at 8 eV [10].

In sodium containing sample we have observed a significant decrease in absorption at 6.5 eV, whereas below 6 eV we have recorded induced absorption at 1.85 eV and broad absorption band in the range 4–6 eV. The last band is observed both at 290 and 80 K, whereas the band at 1.85 eV is observed only at 290 K. The coloration due to 1.85 eV band disappeared during 1 h at 290 K.

The investigation was dedicated to revealing the mechanisms of the electronic process responsible for photosensitivity at 290 and 80 K, which are obviously dependent on the nature of the dopant.

Fig. 1. Absorption spectra of silica with aluminum doping (0.025 wt%) at 290 K before and after irradiation with ArF laser pulses. Inset: Induced absorption spectra (difference between irradiated and unirradiated sample) for irradiation at 293 and 80 K. Each sample was annealed at 900 K before irradiation.
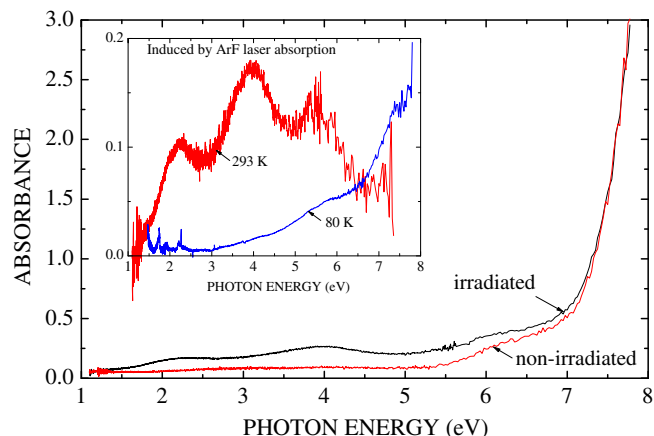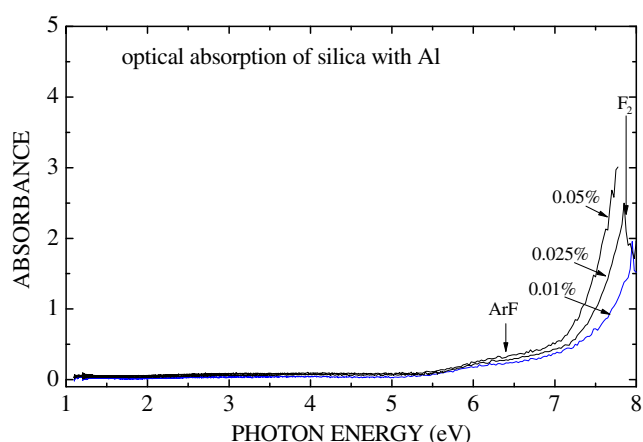
Fig. 2. Absorption spectra of silica with sodium doping (0.025% wt%) at 290 K before and after irradiation with ArF laser pulses. Inset: Induced absorption spectra (difference between irradiated and unirradiated sample) for 293 and 80 K. Each sample was annealed at 900 K before irradiation.

3.1. Luminescence of silica doped with Al

Samples of silica with different concentrations of Al possess structureless optical absorption monotonically increasing up to the optical gap. The absorption is everywhere higher for higher concentrations of Al, Fig. 3. The Al impurity causes an increase of luminescence at 80 K with two bands: a blue one and one in the UV Fig. 4. The blue PL band is situated at 2.6 ± 0.1 eV and UV band at 4.2 ± 0.2 eV. Blue band intensity increases with the concentration of aluminum. Significantly, such spectral shapes of the luminescence are usual for oxygen deficient silica glass without impurities [5,13].

The blue band decay kinetics curve is presented in the insert of Fig. 4 for time range of millisecond and in Fig. 5 for time range of hundreds of seconds. These data in the figures are measured by the photon counting method. The sample exhibits high intensity afterglow during hundreds of seconds after switching off the laser. The long duration decay exhibits the property of weak dependence of the shape of decay curve on temperature. The power law is $\sim t^{-1}$ independently of the temperature Fig. 5. An experiment was performed to check decay behavior with temperature. The sample was heated to 150 K and irradiated with laser. The intensity of luminescence drops down relatively to 80 K irradiation. So, we
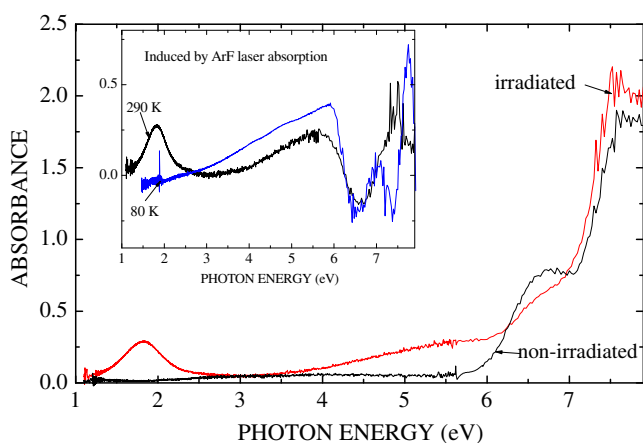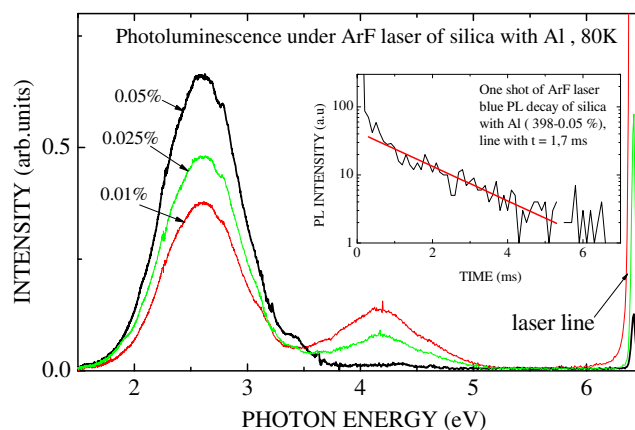

Fig. 4. Photoluminescence of silica glass samples doped with aluminum under ArF-laser excitation. Shown are the spectra for samples with three different Al_2O_3 concentrations (given in wt%). Inset: Blue band (2.7 eV) decay kinetics curve after one laser shot, measured with photon counting method by multichannel analyzer. $T = 80$ K (For interpretation of the references to colour in this figure legend, the reader is referred to the web version of this article.).
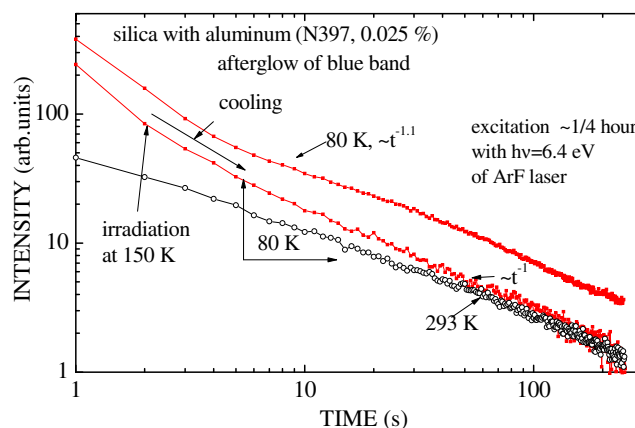

Fig. 5. Blue band afterglow of a silica sample doped with 0.025 wt% of aluminum following ArF irradiations for 1 min at 80 K and 290 K (upper and lower curves, respectively). Middle curve corresponds to irradiation at 150 K and cooling during afterglow measurement to 80 K. the middle curve asymptotically approaches the lower curve, with both curves approaching a $1/t$ (second order kinetic) decay law (For interpretation of the references to colour in this figure legend, the reader is referred to the web version of this article.).

have over-barrier recombination. Beside we have another process less dependent on temperature. Indeed, after few seconds of decay the sample was cooled to 80 K in a time short compared to the decay constant at 80 K Fig. 5. Cooling process does not affect the decay curve. If recombination of charge carriers takes place in thermally stimulated process, the intensity of afterglow should diminish. So, we have direct observation of tunneling recombination of charge carriers. Heating of the irradiated sample gave rise to thermally stimulated luminescence (the blue band was detected). The peak position at 180–200 K, Fig. 6, correlates well with thermal liberation of self-trapped holes [14]. Liberated STHs recombine with trapped electrons. Because we observe blue band evidently belonging to some ODC [4,5], we have additional proof of ODC working as an electron trap in silica. So under irradiation with ArF laser we saw recombination luminescence of ODC, where as a rule the blue band is prevailing.

Let us consider properties of the UV band in silica doped with Al. It is known that UV band is fast [13], better observable in intra-center transition and not developed in recombination luminescence
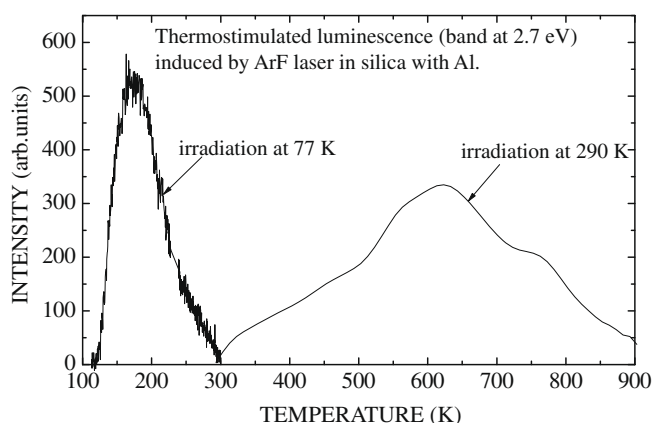

Fig. 3. Optical absorption at 298 K of non-irradiated silica glass samples doped with aluminum. Shown are the Al_2O_3 concentrations in wt% and positions of ArF and F_2 laser photons.

Fig. 6. Thermally stimulated luminescence at 2.7 eV ('blue band') induced by ArF laser in silica with aluminum doping. Noisy curve corresponds to irradiation at 80 K, smoothed curve corresponds to irradiation at 290 K. high and low T curves are measured on different equipments, however, the intensities are visually comparable (For interpretation of the references to colour in this figure legend, the reader is referred to the web version of this article.).

Fig. 8. UV PL decay kinetics of silica with aluminum under ArF laser excitation at different temperatures. Insertion – temperature dependences of UV PL intensity, determined as integral under decay curve, $I(T)$ and decay time constant $\tau(T)$.

[4,5,9]. So we have studied fast luminescence of silica doped with Al, Fig. 7. Analyses of time-resolved luminescence reveal the center to comprise twofold coordinated silicon (oxygen deficient center or ODC) with the characteristic 4.5 ns decay time of the UV emission band corresponding to singlet–singlet transitions of the center [13]. The decay of the slow triplet–singlet blue band of this center is obscured by strong recombination luminescence, so we were not able to detect pure intra-center decay of the blue band with characteristic time constant equal 10.3 ms [13]. Beside the fast component of decay with time constant 4.5 ns, we have observed as well the decay of the UV band in the microsecond range, Fig. 8, which obviously corresponds to a part of recombination excited ODC luminescence in this time range. Acceleration of decay rate with increase of the temperature and practical independence of intensity is observed and demonstrates over-barrier recombination of defects. Participation of UV band in long duration afterglow takes place as well.

3.2. Electron spin resonance of silica doped with Al

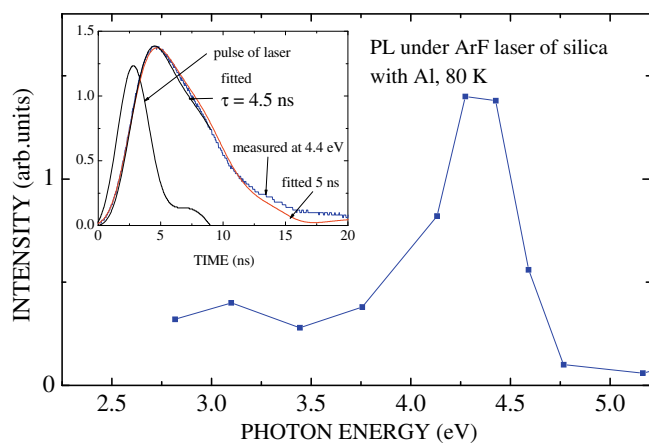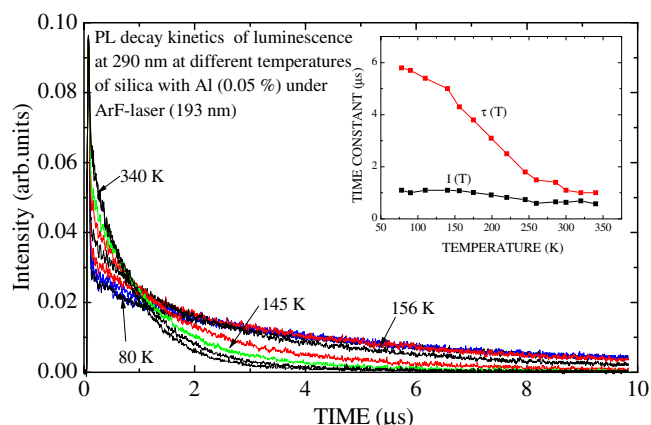ESR spectra are presented in Fig. 9 for silica glass doped with Al irradiated at 80 K and measured also at 80 K. Spectra correspond-ing to irradiation at 290 K are presented in Fig. 10. Significant dif-ferences in ESR signal were observed for irradiation at 77 K compared with 290 K. At 77 K the self-trapped hole (STH) signal [14] is recorded, whereas at 290 K the well known signals of Al–oxygen hole center (Al–OHC) [15] and E' center were observed. This result is in agreement with observation of induced absorption bands at 2.3 eV (Al–OHC) and 5.5 eV (E' center).

Those signals that remained stable at room temperature were also recorded in both (1) the slow-passage first-derivative mode and (2) the fast-passage high-power second-harmonic mode on a computer-controlled Bruker spectrometer Fig. 11. Measurements in mode (1) permitted determinations the following spin-concen-trations: Relict Si–E' centers in an unirradiated Al-doped sample ($\sim1.5 \times 10^{14}$ spins/cm^3); ArF-laser-induced Si–E' centers in an Al-doped sample (9.8×10^{15} spins/cm^3); Ar-laser-induced Al–OHC in an Al-doped sample ($\sim2 \times 10^{16}$ spins/cm^3). In addition, it was shown that virtually identical Si–E' and Al–OHC spin concentra-tions could produced by X irradiation in a control sample compris-ing fused 'dry' natural quartz containing Al and alkali impurities. This material ('QC') was extensively studied and reported in great-er detail elsewhere [16].

In Fig. 11, the ArF-laser-irradiated Al-doped silica of this study was recorded in mode (2) with comparison to the X-irradiated QC glass. Here, in addition to the Si–E' center mostly manifested

Fig. 7. Time resolved PL spectrum, where intensities at several discrete photon energies were determined by integration of PL pulses in time range 0 – 20 ns of Al-doped silica glass induced by an ArF laser pulse. Inset: Shape of PL pulses for UV band (4.4 eV) compared with fitted by convolution of laser pulse with correspond-ing exponent. T = 80 K.
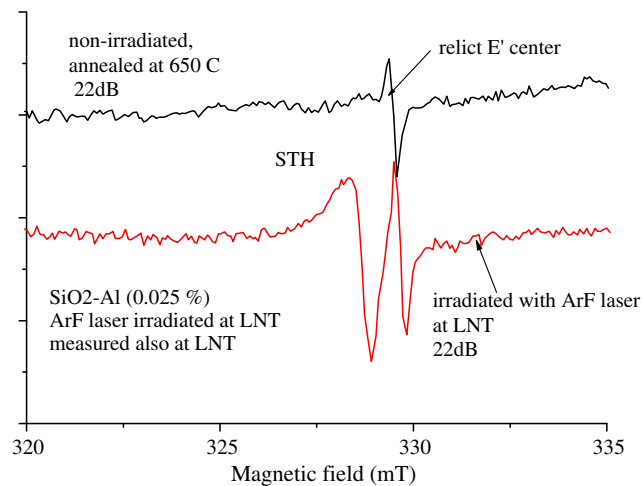

Fig. 9. ESR spectrum of silica with Al (0.025%) ArF laser irradiated and measured at LNT (lower) with comparison to unirradiated also measured at LNT (upper).
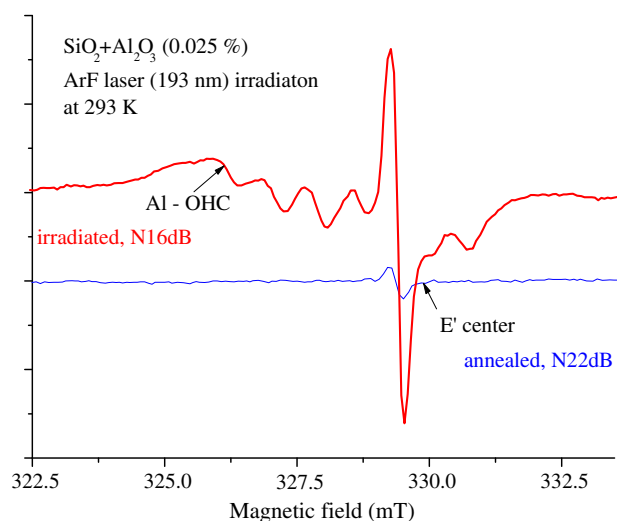
Fig. 10. Silica with Al (0.025%) irradiated with ArF laser (193 nm) at 293 K (lower) with comparison to an unirradiated sample also measured at 293 K (upper).
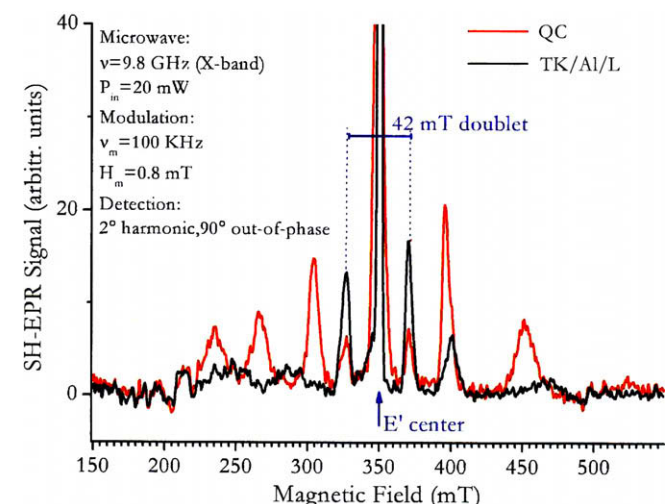

Fig. 11. High-power second-harmonic mode spectra of the Al-doped, ArF-laser-irradiated sample of this study (black signal) with comparison to sample QC, a silica glass prepared from fusion of natural containing Al and alkali impurities but <1 ppm by weight of OH (red signal). The six-line ^{27}Al hyperfine spectrum of QC is typical of Al-EC-type centers charge compensated by Li$^+$ or Na$^+$ ions [17,18], whereas the broader, larger-coupling-constant lines are consistent with Brower's results for Al-doped silicas wherein the alkali ions had been replaced by protons by means of high-temperature electrolysis [18].

as the central line (off scale in both cases) and its ^{29}Si hyperfine structure (the indicated 42 mT doublet), we observe six ^{27}Al hyperfine lines (one of them overlapping the central Si–E' center line). Brower [17,18] has proved that the ^{27}Al features seen in the QC glass are due to Al-E' centers [17,18]. The ^{27}Al structure of the presently studied ArF-irradiated Al-doped silica is substantially different, and possible implications of this difference will be discussed in Section 4.

3.3. Luminescence of silica doped with Na

Photoluminescence spectra of silica glass samples doped with sodium are presented in Fig. 12. A broad luminescence band at 3.5 eV with FWHM about 1.2 eV and a shoulder at 2.5 eV, as well as a band at 1.9 eV with FWHM about 0.2 eV, are observed under ArF laser excitation. The band at 3.5 eV weakens while the band at 1.9 eV grows stronger with irradiation time. There is good corre-
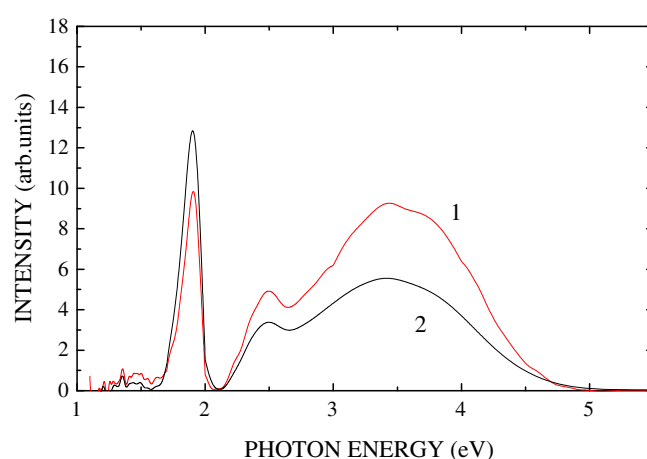
spondence between band at 3.5 eV in Na-doped silica and that of sodium silicate glasses containing up to 25 mol% Na$_2$O, known from previous investigation ([4] and references therein). Red luminescence of Na-doped silica correlates well [19] with a radiation defect of silica glass known as nonbridging oxygen hole center (NBOHC) in pure silica, or as HC$_1$ or HC$_2$ in alkali silicate glasses [20,21].

Decay kinetics curves of Na-doped silica glass and sodium silicate glasses are compared in Fig. 13. Here, it is seen that not merely the positions of the PL bands but also the decay kinetics curves are similar for these two materials. Previously, the decay kinetics of sodium silicate glass in this range of time was interpreted as intra-center triplet-singlet transitions in a structure $\equiv$Si–O$^-$–Na$^+$ named as L-center [4]. In addition to the intra-center process of photoluminescence excitation in sodium silicate glasses, a rich picture of recombination processes was also observed [4]. Presently, we have measured decay kinetics over a longer time range, as well for Na-doped silica glass, Fig. 14. The upper curve in Fig. 13 unequivocally indicates an over-barrier recombination process (liberation of the charge carriers into energy bands followed by recombination on recombination centers) resulting in an afterglow approaching a power law $\sim t^{-2}$ at long times, whereas the decay obtained by irradiation at high temperature followed by quick cooling suggests tunneling recombination weakly dependent on temperature. These processes previously were investigated in detail for sodium silicate glasses in [22].

Fig. 12. Photoluminescence under ArF laser irradiation of silica samples with sodium doping (1–0.025% and 2–0.05%) at 290 K.
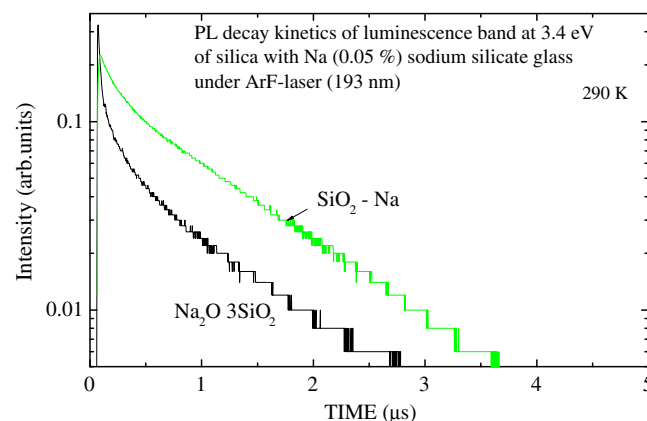

Fig. 13. PL decay kinetics of the luminescence band at 3.5 eV of silica doped with 0.05% Na with comparison to that of sodium silicate glass (Na$_2$O·3SiO$_2$) under ArF-laser (193 nm) at 290 K. The decay kinetics curves are measured with oscilloscope and photomultiplier FEU-106.
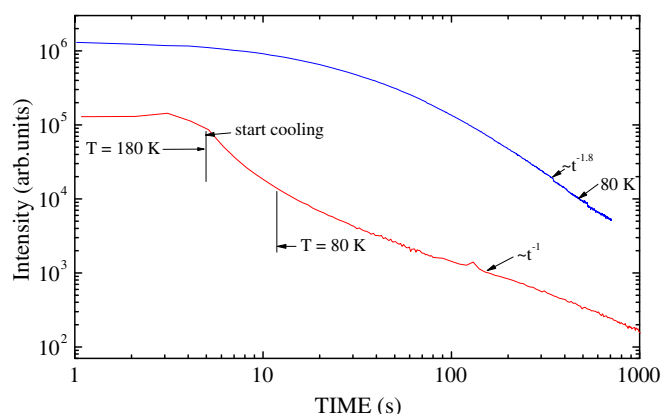
Fig. 14. PL decay kinetics of the luminescence band at 3.5 eV of silica doped with 0.025% Na under ArF-laser (193 nm) irradiation. Upper curve was measured at 80 K after irradiation at 80 K. The curve below was obtained by irradiation at 180 K with subsequent cooling to 80 K in ~10 s. The curves are presented as received, reflecting lower luminescence intensity at 180 K than at 80 K.
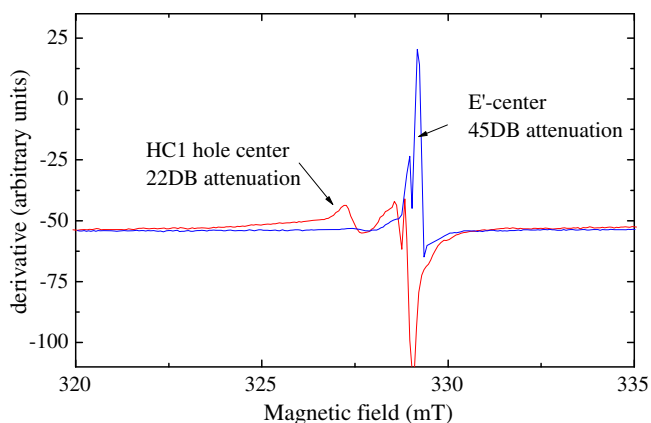

Fig. 15. ESR spectra of ArF-laser irradiated silica glass doped with 0.05 wt% of sodium irradiated at at 290 K and measured at 80 K.

3.4. Electron spin resonance of silica doped with Na

The results of ESR measurement of silica glass doped with sodium are presented in Fig. 15. One result of high microwave power is to diminish the E' center signal due to saturation, so the observed signal corresponds mostly to the HC_1 center [20,21]. At low power detection of E' center is more favorable (although its line shape at 45 dB is still seriously distorted by rapid-passage effects). Thus, irradiation of Na-doped silica glass leads to observation of two trapped-hole-type centers, Si–E' and HC_1. The corresponding electron traps in these glasses are ESR silent for unknown reasons. ArF-laser irradiation at 80 K resulted mainly in the signal of HC_1 center but with smaller concentration than that for 290 K. Si–E' centers may or may not be created at low temperature; (the E' center signal actually observed is at least partially a relict of earlier irradiations that was not totally removed by annealing prior to performing the present experiment).

4. Discussion

4.1. Radiation effects in silica doped with Al

The main results obtained in this research derive from the differences of radiation-induced properties at 290 and 80 K of silica doped with aluminum consequent to irradiation with photons of

ArF laser (~6.4 eV). The states related to aluminum oxide are situated higher than optical gap of silica [10] and do not absorb laser irradiation directly. That is, the differences in induced optical absorption and electron spin resonance. At room temperature we have observed induced optical absorption bands not unexpected for aluminum-doped silica. These are bands at 2.25, 4.1 and 5.5 eV (inset to Fig. 1, red curve).[1] The first of these bands belongs at least in part to Al–OHC, that is, a hole trapped on oxygen atoms of an AlO_4 tetrahedron [23]. The Al–OHC is best known from studies of α quartz (see [23] for optical spectra and [24] for a review of ESR studies and analyses), but it has also been demonstrated in glassy silica [15,25]. The lower ESR signal of Fig. 10 well replicates the Al–OHC spectra reported for Al-doped silica glasses [15,25]. The optical band at 4.1 eV also accompanies presence of aluminum irradiated silica glass and quartz [23], whereas the one at 5.5 eV likely belongs to the Si–E' center since a band at 5.4 eV in irradiated α quartz [26] has been correlated with the Si E_2' center in quartz [27] and an Si–E'-center ESR signal is observed in Fig. 10.

At 80 K we have observed structureless spectra of induced optical absorption manifested as monotonically increasing absorption coefficient with increasing photon energy (inset to Fig. 1, blue curve). In the ESR spectrum of the sample irradiated at 80 K, a signal of the self-trapped hole (STH) was detected, Fig. 9. (The accompanying signal of E' center in Fig. 9 is at least partially due to the relict signal of a previous irradiation, which was not possible to anneal even at 900 K.) Therefore, it might be guessed that excitation of the electronic states takes place in regions of the silica glass network far from Al impurities and precursors of the E' centers, since thermal release of STHs and diffusion of the holes followed by trapping on four-coordinated Al or on precursors of the Si–E' center provides corresponding defects at room temperature. Corroborating this notion is the fact that Amosov et al. [28] observed what in hindsight was certainly the spectrum of STHs upon irradiating an impure (but 'dry') silica sample at 77 K, and this STH spectrum was replaced by the spectrum of Al–OHCs upon warming to 300 K.

Still, there is reason to believe that many of the ArF-laser-excited states may be directly connected with oxygen deficient centers, to the extent that ODCs are responsible for the continuous absorption of the localized states (Fig. 3) below the photoconductivity band gap of amorphous SiO_2, ~9 eV [29,30]. This premise is strongly supported by the luminescence data.

The photoluminescence (PL) of studied samples exhibits similar behavior both at 290 and 80 K with only slightly different intensities; (only the 80 K data are shown in Fig. 4). In both cases the main band in the stationary regime of detection is the broad blue band at 2.7 eV, accompanied by a not-so-well-defined UV band in the range of 4–4.5 eV. The time resolved PL spectra of Fig. 7 show that the luminescence may arise from several processes. One of them is intra-center process. Observation of the UV PL band with well defined position at 4.4 eV with time constant of 4.5 ns (Fig. 7) unequivocally identifies this luminescence as that of a particular oxygen deficient center, ODC(II) – the twofold coordinated silicon [13,31,32]. This emission band corresponds to the allowed singlet–singlet transition of this center. However, the corresponding 2.7-eV triplet–singlet transition blue luminescence with time constant 10.2 ms [13,31,32] was not observed. Therefore, we conclude that oxygen deficient center is twofold coordinated silicon modified by its surroundings; (with regard to the possible modified natures of this center see, e.g., discussions in [4,5,9]). The presently observed luminescence is believed to result when a transient twofold-coordinated silicon is created from the initial 'modified' center. The surroundings of this local complex relax only a small

---

[1] For interpretation of color in Fig. 1, the reader is referred to the web version of this article.

distance. Back relaxation of these surroundings kills the ability of the center to provide luminescence. In such a way the intrinsically slow blue luminescence appears to be fast. Meanwhile, the intrinsically fast UV luminescence has time for radiative transitions in 'normal' way during the lifetime of transient photo-transformed modified twofold coordinated silicon. Thus, we see decay kinetics directly related to the lifetime of transient photo-structural transformations.

We observe a wide spectrum of decay kinetics with lifetimes ranging from 0.2 μs–1.7 ms to the power-law afterglow of Fig. 5 lasting minutes. The observed thermally stimulated luminescence of Fig. 6, where main band is the 2.7 eV blue band, is believed to be witnessing directly a recombination process involving isolated STHs diffusing to the sites of modified ODCs(II):e^- [6]. Consistent with this view, when irradiation was performed at higher temperature and the sample was cooled during measurement of the decay curve, the luminescence intensity was unaffected, Fig. 5. This, together with decay following a t^{-1} law [22], is evidence for tunneling recombination between a trapped electron of a modified ODC(II)e^- and a nearby hole. As proven in Fig. 9, the hole is self-trapped at 80 K. The corresponding electron therefore must be trapped somewhere nearby the luminescing ODC, since 6.4 eV ArF photon excitation must leave the hole h^+ and electron (e^-) trapped above (below) its respective mobility edge [1,33].

Otherwise, the UV band, besides a fast decaying PL component, exhibits a slow component, Fig. 8, which is obviously not due to intra-center transitions. There are strong changes of decay time constant with temperature, yet the UV band intensity is practically independent of temperature (figure omitted). These effects are easy to understand in the framework of recombination processes. Increasing detrapping of STHs with increasing temperature in the range ~80–250 K [14,34] increases the rate of recombination. Previously we have observed analogous recombination luminescence processes [35]; however, until now we had not the possibility to check in the associated ESR spectra.

4.2. Why the Al-doped samples tell us far more than the oxygen deficient pure silicas

Previously [9] it was shown that oxygen deficiency stimulates hole self-trapping. As reviewed in [9], *the trapped electrons in high purity, but oxygen deficient, silicas are ESR silent.* No ESR spectrum identifiable as that of a trapped e^- has ever been reported in these materials. Thus, if we investigate oxygen-deficient silicas only, we are left deaf and blind to all processes involving excited electrons, e^-.

By contrast, we know from the work of Brower [17,18] that the spectra of Fig. 11 exhibit ^{27}Si hyperfine structure (hfs) due to electrons paradoxically trapped on Al^{3+} ions in a glass network comprised mainly of Si^{4+} ions in tetrahedral coordination by O^{2-} ions. Brower [17,18] made an extremely persuasive case that pre-existing three-coordinated Al^{3+} ions ($AlO_{3/2}^0$ structures) trap electrons during irradiations at cryogenic temperatures and that small percentages of them become stabilized at or above 300 K upon the arrival by diffusion of charge compensating alkali ions or protons. Brower found the measured values of the ^{27}Al isotropic hyperfine coupling constants, A_{iso}, to depend on the nature of the charge compensator [18]. And he further noted that the four-coordinated Al^{3+} ions, which upon hole trapping become Al–OHCs, must themselves have been charge compensated by interstitial ions in his less-pure samples. And he produced evidence that these compensators diffuse away from tetrahedral Al^{3+} sites after hole trapping there, with some of these mobile ions becoming available to charge compensate the trapped-electron centers. (As reviewed in [15], these are exactly the kinds of process that take place in α quartz – except that, unlike virtually all other known defects in glassy SiO_2, Brower's 'Al E' centers' do not occur in α quartz!)

This is the paradox: Why would a an ion (Al^{3+}) that is less-electronegative than Si^{4+} serve as a stable electron trap in a glassy SiO_2 network, especially given that such a thing doesn't happen in quartz?

4.3. A model-independent summary of radiation-induced processes in the Al-doped sample

Aluminum-doping apparently emulates the effects of high ODC concentrations in pure silicas, that is, both the observed absorption in the range ~5–9 eV (Fig. 3) and the PL at 2.7 eV (Fig. 4) are 'amplified' relative to the pure glass. Thus, the optical absorption of the non-irradiated Al-doped samples presented in Fig. 1 corresponds to wide spectrum of ODC-like localized states progressively 'amplified' with increasing Al content. Previously we have observed the recombination luminescence process for Al-doped silica [10], but this is the first time we have been able to check the ESR at the same time.

Excitation with ArF laser light was performed without use of focusing lens, so all of the data we present here resulted from single-photon processes. In the absorption spectrum of the unirradiated sample Figs. 1 and 3, there is no specific absorption band. We observe only monotonic increase of absorption coefficient. There is no specific absorption band of aluminum. All such bands are lying higher. Absorption of light takes place within localized states of silica glass, which manifest themselves through ODCs of many different kinds. These states work as energy absorbing entities. Separation of charge carriers takes place in a multi-step process on different distances. The main recombination process involves recombination of these separated charge carriers in non-thermally-activated process at low temperatures. At high temperature, when self-trapped hole is easy liberated, other holes centers such as the E' center and the Al–OHC may be created and can be detected optically or by ESR.

The radiation processes in silica with Al can be viewed as a cascade of reactions:

(1) Localized States + $h\nu$(6.4 eV) ⇒ (LS)* = (ODC)* + modifier

(2) Intra-center luminescence of the twofold-coordinated silicon centers created by irradiation: blue (2.7 eV) & UV (4.4 eV) bands

(3) Photon assistant ionization of (ODCs)* + modifier with creation ODC$^-$s and STHs on different distances.

(4) Low-T tunneling recombination of ODC$^-$s with closest STHs

(5) Thermal release of STH and migration to ODC$^-$s on a longer distance, preventing tunneling recombination giving rise to TSL at ~200 K

(6) $T > 200$ K STH migration and trapping on AlO_4 and Vo structures:

$$STH + [AlO_4]^- \Rightarrow [AlO_4]^0; STH + Vo \Rightarrow E'.$$

Creation of TSL peak at 600 K.

In the same time: $\equiv Si^+ Al\equiv + e^- \rightarrow \equiv Si^+ Al^{-}\equiv$ for irradiation at 290 K presumably with induced absorption band at 4.1 eV.

Thus, ODCs play the role of electron traps, which increase STH production as concluded previously [9].

Apparently, the Al impurity alone in silica (not accompanied with alkali ions) stimulates oxygen deficiency center concentrations or concentration of localized states that also act as electron traps. As proposed in [11], aluminum oxide electronic transitions likely lie at higher energy than the optical gap of silica. We observe rich phenomena of recombination processes taking place as tunneling recombination at low temperature. At high temperatures, beside recombination processes with higher rates than at low

temperature, we observe recombination of defects mobilized at 600 K. ODC luminescence is observed also in this case. Color centers associated with aluminum are also annealed by heating, so we propose the existence of deep electron traps on ODCs and/or defects related to ODCs.
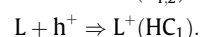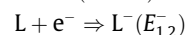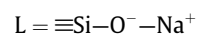
4.4. Radiation processes in silica doped with Na

Sodium-doped silica irradiated with pulses of ArF laser light exhibits changes in optical absorption. In Fig. 2, the broad band at 6.8 eV (FWHM ~1 eV) in the unirradiated sample is ascribed to the so-called L-center associated with the cluster Si–O⁻–Na⁺, as known for sodium silicate glasses [4,36,37]. So, it could be directly excited with ArF laser's photons. It is also seen in Fig. 2 that the pre-existing L band is diminished in intensity during irradiation. The induced absorption band at 1.82 eV (FWHM ~0.6 eV), known for sodium silicate glasses as the $E_{1,2}^-$ centers [36], was induced together with broad complicated band at 5.6–5.7 eV containing a sub-band at 4.7 eV. The band at 1.82 eV decays during 1 h, but induced bands at 4.7 and 5.7 eV remain stable. The photoluminescence spectra of Fig. 12, measured during irradiation show broad band at 3.5 eV of L-center, a shoulder at 2.5 eV, and a band at 1.9 eV. The 1.9 eV band, certainly due to alkali-associated nonbridging-oxygen hole centers (certainly HC₁ and perhaps HC₂ [20,21]), grows during irradiation from an initially negligible level.

The ESR spectra of Fig. 15 show a peculiarly broadened Si–E' center contribution, possibly due to hyperfine interactions with a nearby ²³Na nucleus ($S = 3/2$, 100% natural abundance). This broadening is ~10 Gauss, which when compared with A_{iso} for the Na atom (~300 G), suggests that the wavefunction of the unpaired electron of this Si–E' center may have about a 3% overlap with a ²³Na nucleus (or nuclei). This result is consistent with the fact that the wavefunction of the E'-type center in a γ-irradiated K₂O–5SiO₂ glass has been unambiguously shown to be ~12% delocalized [38], presumably onto potassium ions.

4.5. Modelling radiation processes in Na-doped silicas

The model of the ionizing-radiation processes is proposed as liberation of an electron from one L center and its trapping on another L center, resulting in the creation of an $E_{1,2}^-$ center (Na⁰) where the electron has trapped and an HC₁ giving red luminescence where the hole has trapped. Main radiation reactions can be represented as:

$$L = \equiv Si-O^- -Na^+$$
$$L + h\nu(6.4\,eV) \Rightarrow L^* \Rightarrow L + h\nu(3.5\,eV)$$
$$L + e^- \Rightarrow L^-(E_{1,2}^-)$$
$$L + h^+ \Rightarrow L^+(HC_1).$$

The efficiency of the reaction $2L + h\nu \Rightarrow L^-(E_{1,2}^-) + L^+(HC_1)$ diminishes with decreasing temperature. To a smaller degree, the hole can be liberated and re-trapped on a precursor of E' center. So, a mixture of centers characteristic of sodium silicate glasses and silica glasses takes place in sodium-doped silica.

5. Conclusions

The main part of the absorbed energy during 6.4 eV ArF laser irradiation of pure silica glass is transformed to instant luminescence. The observed afterglow and thermally stimulated luminescence both correlate with specific induced color centers. The luminescence of pure silica glass contains only the bands of ODC(II), the twofold coordinated silicon center. However, these ODCs(II) are strongly modified by their immediate surroundings.

Sodium doping completely changes picture related to localized states in that sodium–oxygen-related states and the phenomena specific to them obscure the optical spectroscopic properties of localized states intrinsic to the pure-silica parts of the glass. By contrast, aluminum-doped silica displays manifestations of localized states which mimic, yet do not strongly exceed, those attributed to ODCs(II) in oxygen deficient pure silica. The radiation properties of silica glass with sodium are strongly connected with Si–O⁻–Na⁺ groupings, called L centers. At room temperature ArF laser radiation falls into lowest energy absorption band of the L center, which promotes an electron from a nonbridging oxygen to a nearby sodium ion. Backward transitions produce intra-center luminescence and carrier recombination. However, if the resulting sodium atom drifts away the intra-center luminescence is quenched, and a stable $E_{1,2}$ center related to Na⁰ is formed a few coordination spheres distant from an HC₁ oxygen-trapped-hole center, which gives a red luminescence.

By contrast, the presence of aluminum impurities in silica unaccompanied by alkali ions is shown here to give rise to localized states capable of trapping electrons, very similar to the role played by oxygen deficient centers (ODCs) in pure silica. The nature of the trapped holes induced by ArF laser irradiation in Al-doped silica at 80 K has been shown by ESR to be self-trapped holes (STHs).

In summary, irradiation of pure and single-cation-doped silicas with ArF laser photons reveals a rich picture of electron and hole release and trapping. It is noted in the studied samples that the radiation processes are different for 290 and 80 K. Whereas at 80 K the ESR signal of STHs is observed, at 290 K the ESR signals of the aluminum–oxygen hole center (Al–OHC) and the E' center are induced, and the induced optical absorption contains the known bands of these centers. A variant of the aluminum electron center (Al–EC) is also observed upon 6.4-eV irradiation at 290 K, probably with optical band at 4.1 eV appears to be associated with it. Therefore, laser excitation of the electronic states may take place in areas of the silica glass network far from Al-impurity and E'-center precursor sites. In this view, thermal release of STHs and diffusion of these holes to the sites of substitutional Al³⁺ ions and ODCs lead to Al–OHC and E' center formation, respectively, at room temperature. The ArF-laser-induced states are directly connected with ODCs in pure silica glasses and with Al-related pseudo-OHCs in Al-doped silica, both of which give rise to continuous absorption of the localized states monotonically rising from <6.4 eV to the optical gap edge at ~9 eV.

References

[1] N.F. Mott, E.A. Davis, Electronic Processes in Non-Crystalline Materials, Oxford, 1971, p. 472.
[2] A.V. Kolobov (Ed.), Photoinduced Metastability in Amorphous Semiconductors, Wiley-VCH, 2003, p. 412.
[3] H.R. Philipp, Solid State Commun. 4 (1966) 73.
[4] A.N. Trukhin, in: G. Pacchioni, L. Skuja, D.L. Griscom (Eds.), Defects in SiO₂ and Related Dielectrics: Science and Technology, Kluwer Academic, London, 2000, p. 235.
[5] A.N. Trukhin, H.-J. Fitting, J. Non-Cryst. Solids 248 (1999) 49.
[6] A.N. Trukhin, T.I. Dyuzheva, L.M. Lityagina, N.A. Bendeliani, J. Phys.: Condens. Matter 20 (2008) 175206.
[7] A. Trukhin, M. Kink, Y. Maksimov, J. Jansons, R. Kink, J. Non-Cryst. Solids 352 (2005) 160.
[8] A.N. Trukhin, J. Non-Cryst. Solids 352 (2006) 3002.
[9] A.N. Trukhin, J. Troks, D.L. Griscom, J. Non-Cryst. Solids 353 (2007) 1560.
[10] A.N. Trukhin, J.L. Jansons, K. Truhins, J. Non-Cryst. Solids 347 (2004) 80.
[11] E.J. Friebele, D.L. Griscom, in: M. Tomozawa, R.H. Doremus (Eds.), Treatise on Material Science and Technology, vol. 17, Academic, New York, 1979, p. 257.

A.N. Trukhin et al. / Journal of Non-Crystalline Solids 355 (2009) 1066–1074

[12] D.L. Griscom, Nucl. Instrum. Methods Phys. Res. B1 (1984) 481.
[13] L.N. Skuja, A.N. Streletsky, A.B. Pakovich, Solid State Commun. 50 (1984) 1069.
[14] D.L. Griscom, J. Non-Cryst. Solids 149 (1992) 137.
[15] D.L. Griscom, in: S.T. Pantelides (Ed.), The Physics of SiO$_2$ and Its Interfaces, Pergamon, New York, 1978, p. 232.
[16] G. Buscarino, PhD thesis, Università di Palermo, 2007.
[17] K.L. Brower, Phys. Rev. Lett. 41 (1978) 879.
[18] K.L. Brower, Phys. Rev. B 20 (1979) 1799.
[19] L.N. Skuja, A.R. Silin, Phys. Stat. Sol. (a) 56 (1979) K11.
[20] D.L. Griscom, J. Non-Cryst. Solids 31 (1978) 241.
[21] D.L. Griscom, J. Non-Cryst. Solids 64 (1984) 229.
[22] A.R. Kangro, M.N. Tolstoi, I.K. Vitols, J. Lumin. 20 (1979) 349.
[23] K. Nassau, B.E. Prescott, Phys. Stat. Sol. (a) 29 (1975) 659.
[24] J.A. Weil, Rad. Eff. 26 (1975) 261.
[25] R. Schnadt, A. Räuber, Solid State Commun. 9 (1971) 159.
[26] C.M. Nelson, R.A. Weeks, J. Am. Ceram. Soc. 43 (1960) 396.
[27] R.A. Weeks, Phys. Rev. 130 (1963) 570.
[28] A.V. Amosov, I.M. Vasserman, D.M. Yudin, in: Proceedings of ninth International Congress on Glass, Paris, 1971, Sect. A1.7, p.707.
[29] T.H. DiStefano, D.E. Eastman, Solid State Commun. 9 (1971) 2259.
[30] D.L. Griscom, J. Non-Cryst. Solids 24 (1977) 155.
[31] L. Skuja, J. Non-Cryst. Solids 239 (1998) 16.
[32] V.A. Radzig, J. Non-Cryst. Solids 239 (1998) 49.
[33] N.F. Mott, Conduction in Non-Crystalline Materials, 2nd Ed., Clarendon, Oxford, 1993.
[34] D.L. Griscom, J. Non-Cryst. Solids 352 (2006) 2601.
[35] A.N. Trukhin, M. Kink, J. Maksimov, R. Kink, T.A. Ermolenko, I.I. Cheremisin, J. Non-Cryst. Solids 342 (2004) 25.
[36] J.H. Mackey, H.L. Smith, A. Haperin, J. Phys. Chem. Solids 27 (1966) 1759.
[37] A.N. Trukhin, J. Non-Cryst. Solids 189 (1995) 1.
[38] R. Cases, D.L. Griscom, Nucl. Instrum. Methods Phys. Res. (1984) 503.